Available online at www.sciencedirect.com
ScienceDirect
Trans. Nonferrous Met. Soc. China 26(2016) 2679−2686
Transactions of Nonferrous Metals Society of China
www.tnmsc.cn

Mechanical properties of Cu matrix composite fabricated by extrusion process

Ji-Hun PAK[1], Gwi-Nam KIM[1], Sung-Gu HWANG[1], Beom-Su KIM[2], Jung-Pil NOH[3], Sun-Chul HUH[3]

1. Department of Mechanical and Precision Engineering, Gyeongsang National University, Tongyeong 53064, Korea;
2. Department of Mechanical System Engineering, Gyeongsang National University, Tongyeong 53064, Korea;
3. Department of Mechanical and Energy Engineering, Gyeongsang National University, Tongyeong 53064, Korea

Received 10 August 2015; accepted 29 April 2016

Abstract: Carbon nanotube (CNT) was applied in various fields for its superior electrical, mechanical and thermal characteristics. After composites were fabricated by extrusion process using ball-milled Cu−CNT powders, mechanical properties of Cu−CNT composites according to CNT fraction were reviewed. CNT (1%, 5% and 10%), Cu (d=100 nm), zirconia balls (90 g) and ethanol (20 mL) were mixed and dispersed for 5 h at a speed of 500 r/min using a planetary ball mill. A billet (d=50 mm, length=100 mm) was made with Cu, and the composite powders were filled up into billet using the uni-axial press. In the extrusion process, after the billet was heated at 880 °C for 1 h, specimens were produced in the shape of a round bar using the billet by applying a load of 200 t. The composite powders were measured for particle size by particle size distribution equipment. Then the specimen surface fabricated by extrusion was observed by SEM. Mechanical properties measured by the indentation equipment increased with increasing CNT content. The yield strength, tensile strength and hardness of the Cu–CNTs composites can be obviously improved.
Key words: carbon nanotube (CNT); extrusion; milling; indentation; matrix; mechanical properties; microstructure

1 Introduction

As the industry develops and advances, studies on high-density and high-strength materials are conducted in various fields. Also, studies on composites are actively conducted, as superior mechanical properties and high performance which could not be obtained from a single material can be obtained by combining several materials [1].

Carbon nanotube (CNT) was discovered by IIJIMA in 1991 [2]. It is an allotrope of carbon, having a nanostructure in a tubular form. The electrical conductivity of CNT is similar to that of copper. Its thermal conductivity is as high as that of diamond which is the best in the natural world, and the tensile strength of CNT is 100 times better than that of steel. Therefore, a wide range of studies have been conducted on mixing CNT to produce new composites with high mechanical strength and electric/thermal conductivity, utilizing its structural diversity [2−6].

In particular, application in the new material development field has led to development of nano composites using the features of CNT of being light but having high strength [5−9].

Cu is a ductile material with good electrical and thermal conductivity, which is widely used in various fields. In the development of composites which can efficiently improve the characteristics of Cu, CNT has a very high potential as a material which satisfies mechanical and electric requirements at the same time. However, nano-size CNT has a bad dispersibility and a tendency to flocculate. Efforts are being made using diverse methods to resolve this problem [10].

As a typical example, studies are conducted adopting the method of dispersing CNT in the base, using ball milling. Ball milling is a mechanical method of crushing and dispersing particles using the friction energy generated between the balls and the particles when balls are put together with particles into a container, which is then rotated [11]. Cost using ball milling is low, because principle of ball milling is simple. This method is widely used across the whole industry. In order to manufacture composites in powder state in bulk form, diverse studies such as vacuum hot press, spark plasma sintering [12], pressureless sintering and plastic working are conducted [13−17].

Extrusion is one of the methods of plastic workings.

Corresponding author: Sun-Chul HUH; Tel: +82-55-772-9111; E-mail: schuh@gnu.ac.kr
DOI: 10.1016/S1003-6326(16)64356-X

It is a processing method of making the cross-sectional area smaller than the original area and manufacturing the product in its desired form by compressing the material in a mold and letting it escape through the outlet of the mold. It is a method mainly used in powder metallurgy and is used to produce diverse materials such as polymers and ceramics [18].

Extrusion is largely divided into indirect and direct extrusion. While it is difficult to apply indirect extrusion in industrial sites due to the accompanying economic and structural restrictions, it is essential to conduct studies on direct extrusion as it is easily applied in production sites as the mold and billet can be relatively easily produced and continuous extrusion is possible.

In this study, composites were manufactured using Cu as the matrix and CNT as the additive. CNTs were dispersed over the Cu base through ball milling (500 r/min, 5 h). The effect of CNT on the mechanical properties of the Cu−CNT composite was studied by measuring strength and hardness, and observing the surface after producing round bar-shaped specimens by way of high temperature extrusion, using the composite material in powder state compressed in a copper can.

2 Experimental

2.1 Production of nano powder

Figure 1 shows a flow chart of the test process. Pure Cu powder (Nano Technology, 99%) with 100 nm in diameter, and 1−5 μm long CNT powder (Carbon nano material technology, 99%) with 20 nm in diameter were used. As CNT was produced by chemical vapor deposition (CVD) method, there were residual catalyst ingredients, which were removed by acid purification process. CNT was put into the solution made by mixing nitric acid (HNO_3) and sulfuric acid (H_2SO_4) at the volume ratio of 1:3, and held for 24 h for reaction before repeating a filtering process to set the pH to 7.

For ball milling, 90 g of 3 mm-diameter zirconia balls were placed in a pot and 20 mL of ethanol was added to form the wet ball-milling conditions. And after conducting ball milling for 5 h at a speed of 500 r/min to adjust the CNT fraction in the Cu nano powder to 1%, 5% and 10%, the material was dried by heating it at 90 °C.

2.2 Canning process

The canning process is classified under two processes. For uniaxial pressing, a billet was produced in the form shown in Fig. 2(a). Next, pure Cu powder and Cu−CNT powder were put into it, and it was pressurized in the direction of the Z axis at 2.94 kN/cm^2. Then, it was fully sealed by welding on the cover. Next, the degassing and sealing processes are as below.

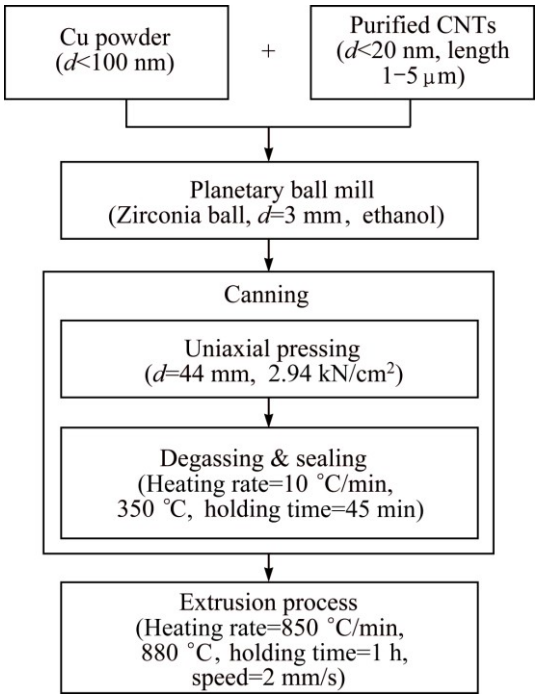

Fig. 1 Flow chart of fabrication procedures of CNT/Cu composites

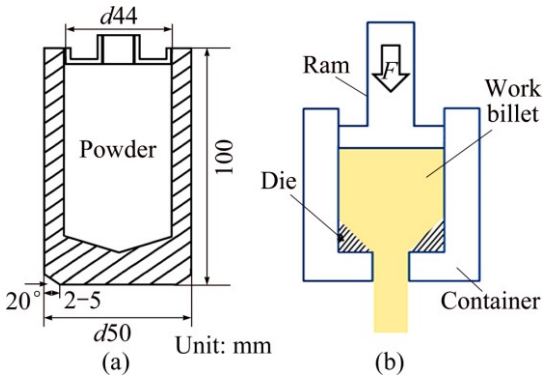

Fig. 2 Schematic diagram of extrusion process: (a) Billet shape; (b) Extrusion processing

The prepared billet was connected to a rotary pump. The oxygen and carbon dioxide inside the billet were removed at 350 °C for 45 min. Then, the connecting part was welded for full sealing.

The filling density of the specimen, calculated after completion of canning, is shown in Table 1. The mass of the powder was obtained by comparing the mass of the

Table 1 Condition of extrusion

Material filled	Can mass/g	Total mass/g	Inside height/mm	Filling density/%
Cu	572.6	1147	74	56.6
1% CNT	565.4	1118.5	74	54.5
5% CNT	583.3	1178.5	74	58.6
10% CNT	601.6	1167.1	74	55.7

empty can and its mass after the powder was filled, and the density was calculated by obtaining the volume of the filled powder. The filling densities of Cu, 1% CNT, 5% CNT and 10% CNT were calculated to be 56.6%, 54.5%, 58.6% and 55.7%, respectively.

2.3 Extrusion process

It is direct extrusion in which the billet is extruded by the pressure generated when the ram of the extrusion equipment descends. A 200 t capacity hydraulic press was used so that the extrusion pressure at each point in time can be measured, as shown in Fig. 2(b).

Extrusion was conducted after maintaining the temperature of the billet at 880 °C for 1 h by way of hot extrusion and placing the billet in a 450 °C container.

Friction between the die and the billet was reduced by setting the die diameter to 16 mm and the extrusion die angle to 20°. In order to reduce friction between the container and the dies, and between the billet and the dies, carbon oil and BN (boron nitride) were applied on the container and billet and dies, as a lubricant.

2.4 Particle size distribution (PSD) test

Dynamic light scattering was used to measure particle and molecule size. This technique measures the diffusion of particles moving under Brownian motion, and converts this to size and a size distribution using the Stokes−Einstein relationship:

$$d_{\mathrm{h}}=\frac{\kappa T}{3\pi\eta D} \tag{1}$$

where d_{h} is hydrodynamic diameter; D is translational diffusion coefficient; k is Boltzmann's constant; T is thermodynamic temperature; and η is viscosity.

2.5 Indentation test

Figure 3 shows advanced indentation system 3000 (AIS3000) by Frontics Inc.. This equipment is approved in ISO/DTR 29381. It consecutively measures the indentation depth by indentation load for a load−deformation curve, and data were analyzed for the mechanical characteristics of the specimen.

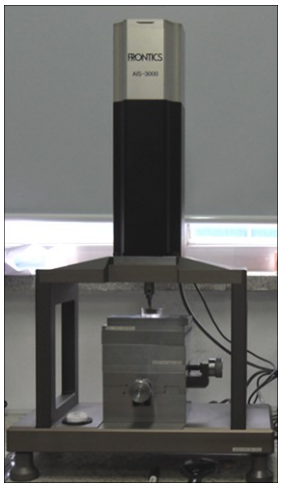

Fig. 3 Indentation test equipment

The algorithm to obtain yield strength and tensile strength is as follows [19]:

$$a\rightarrow a_{\mathrm{c}} \tag{2}$$

where a_{c} is contact area, and it was measured by indentation test.

$$\begin{cases}\sigma=\dfrac{L}{\pi a^2}\dfrac{1}{\psi},\\ \varepsilon=\dfrac{\alpha}{\sqrt{1-(a/R)^2}}\dfrac{a}{R}=\alpha\tan\gamma\end{cases} \tag{3}$$

where L is indentation load; R is the radius of the spherical indenter; ε is the true strain; and ψ and α are default values (α=0.14 and ψ=3.0). Stress−strain points were determined by Eq. (3).

$$\sigma=K\varepsilon^n \tag{4}$$

$$\sigma=K_1\varepsilon^{n_1}+\exp(K_2+n_2\varepsilon) \tag{5}$$

where K is the strength coefficient; n is the strain hardening coefficient. If material is BCC, σ is calculated as Eq. (4). If material is FCC, σ is calculated as Eq. (5). Stress−strain curves are created from stress−strain points by

$$\sigma_{\mathrm{y}}=K(\varepsilon_{\mathrm{y}}+b)^n \tag{6}$$

$$\sigma_{\mathrm{UTS}}=Kn^n \tag{7}$$

where b is material constant.

As to details of the multiple indentation test conditions, the spherical indenter size was d0.5 mm. The maximum indentation depth was set to 150 μm and the indentation speed was 0.3 mm/min. The indentation test was repeated 15 times at every 10 μm, until the load was removed by up to 50% of the maximum load.

3 Results and discussion

3.1 Extrusion pressure result

Figure 4(a) shows the extrusion pressure curves of Cu−CNT composites for different fractions of pure and ball-milled Cu and CNT. The gentle curve which appears at the beginning shows that, with the time increases, there is almost no change in the pressure as the density in the empty space between the container and the billet and inside the billet is increased.

However, in the case of Cu−CNT composite powder, it can be confirmed that the pressure rose more in the same amount of time. The pressure was shown to be 893 MPa in the case of Cu, and shown to have the

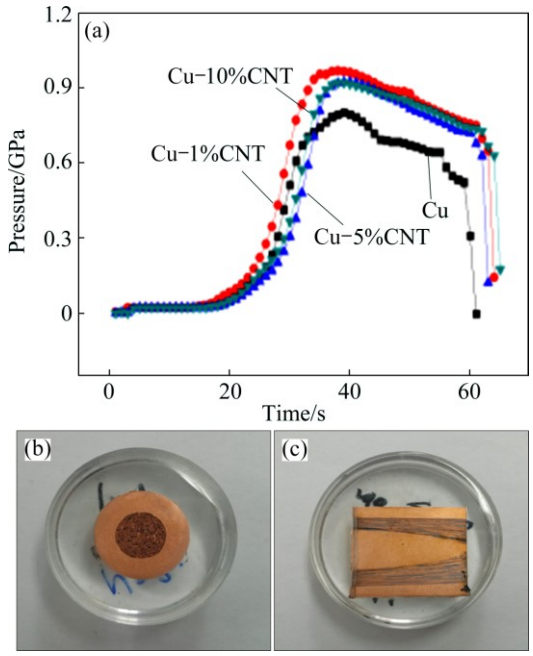

Fig. 4 Results of extrusion test: (a) Extrusion curve; (b) Photograph of longitudinal section; (c) Photograph of cross-section

highest values of 970 MPa, 925 MPa and 923 MPa in the cases of 1% CNT, 5% CNT and 10% CNT, respectively, and decreased later as extrusion progressed. The pressure was higher by 150 MPa in the case that CNT was contained rather than Cu, and the pressure showed a decreasing trend as the CNT fraction increased.

Figures 4(b) and (c) show photographs of the extruded specimens cut in cross-section and longitudinal section for observation, respectively. As the center part is extruded first in the extrusion process, nano powder is observed in the center part at first and in the part relatively near the edge later.

3.2 PSD measurement result

Figure 5 shows the result of measuring the particle size (r) of the powder which contains Cu powder and CNT. The particle sizes of Cu, 1% CNT, 5% CNT and 10% CNT were measured to be 274, 2222, 2815 and 1325 nm, respectively. The Cu particles cluster together due to its ductile property during the ball-milling process, and the particle size is shown to have increased about two times. In the case of the Cu−CNT composite powders, the particle size has increased during the ball-milling process. The particle size of the 5% CNT powder is the biggest.

3.3 Results of powder observation

In order to observe the micro structure of the extruded specimen, the surfaces of specimens were observed using FE-SEM. The specimen was etched for 30 s using a solution made by mixing 24 mL of distilled water, 6 mL of hydrochloric acid and 2 g of iron chloride, and dried immediately after cleaning in distilled water using an ultrasonic cleaner for 10 min. Figure 6

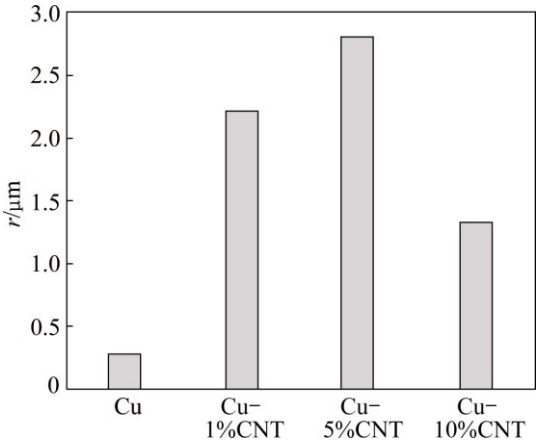

Fig. 5 Size measurement graph of nano powders

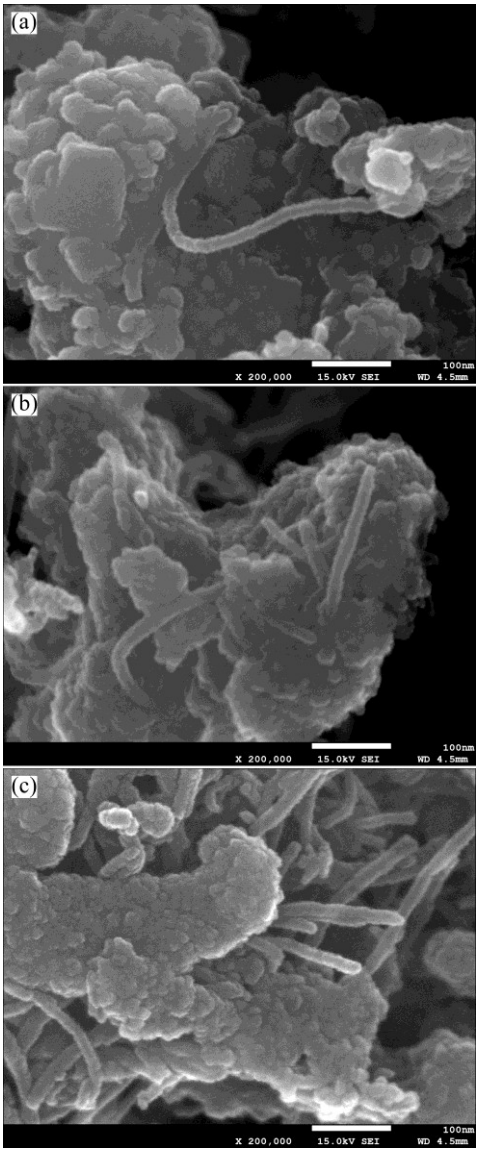

Fig. 6 SEM images of Cu−1%CNT (a), Cu−5%CNT (b) and Cu−10%CNT (c) composites

shows SEM image of the Cu−CNT composite powder using FE-SEM. Figure 6(a) shows that CNT was added in the lump of Cu, while Figs. 6(b) and (c) show that the observed number of CNT rises as the mass of CNT is increased. Therefore, ethanol and CNT were not influenced by the density gap.

Figure 7 shows the result of observing the extruded specimen using FE-SEM after etching the surface of the longitudinal section. Sintering has been done uniformly well as a whole, and air pores are observed.

It seems that the particles of the CNT specimen are smaller than those of the Cu specimen. While the particle size seems to gradually increase as the CNT fraction increases up to 5%, the particles of the 10%CNT specimen seem to be smaller, and particles in the form of powder are still observed. This is because a high CNT content rather interferes with crystal growth, and that CNT content has a major influence on the particle size of the specimen.

Figure 8 shows the result of the observed surface of

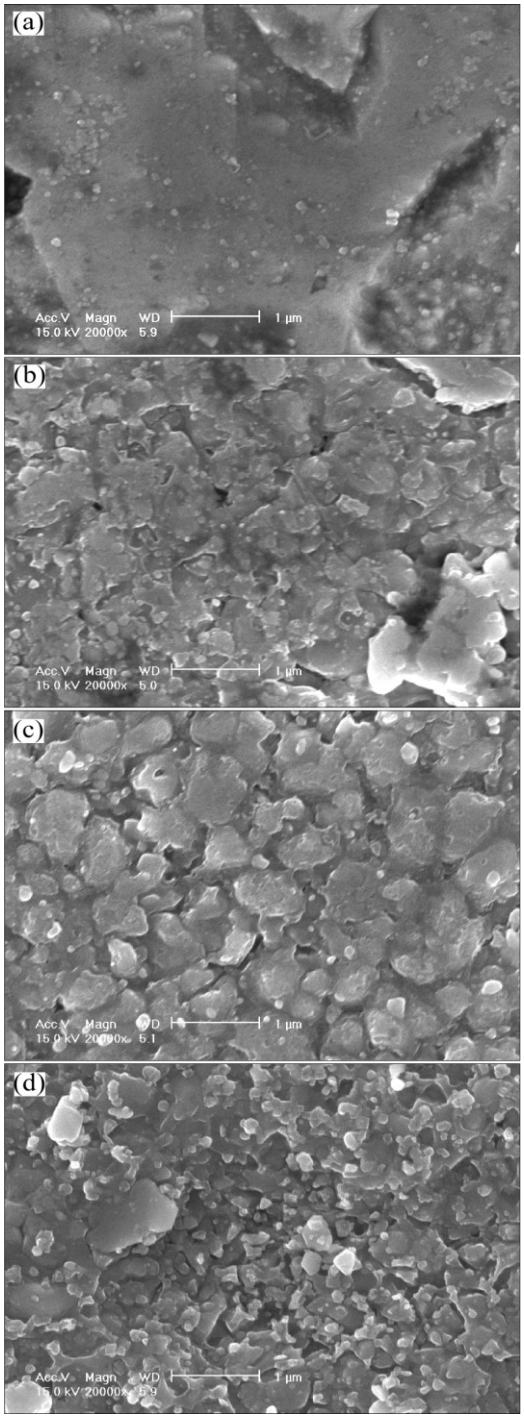

Fig. 7 SEM images of Cu and Cu−CNT etched longitudinal section surface: (a) Cu; (b) Cu−1%CNT; (c) Cu−5%CNT; (d) Cu−10%CNT

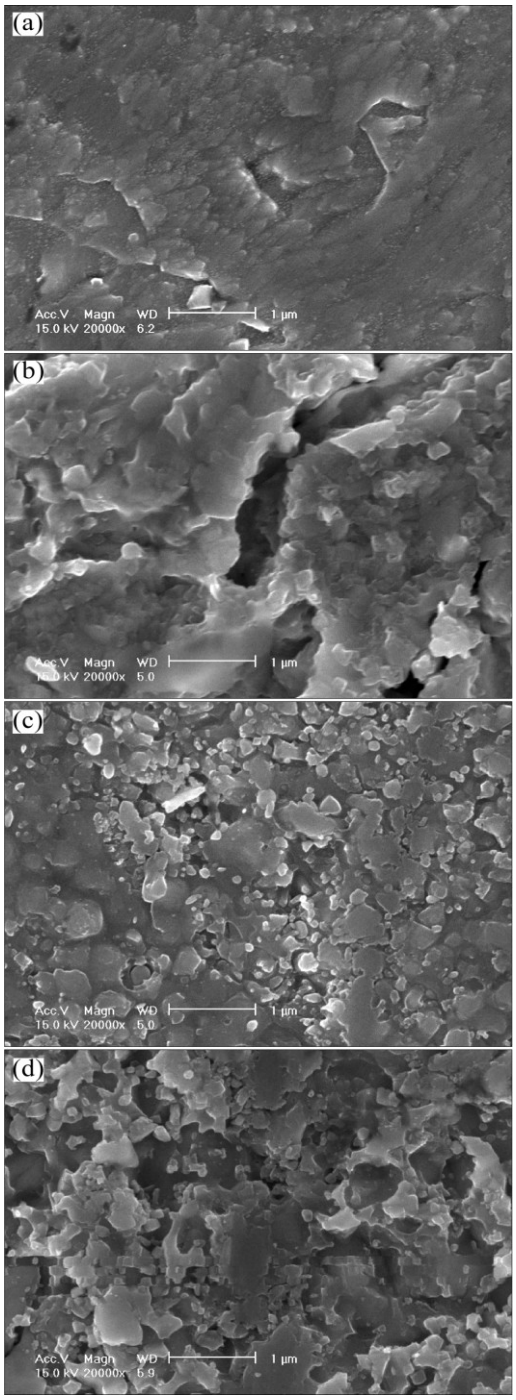

Fig. 8 SEM images of Cu and Cu−CNT etched cross-section surface: (a) Cu; (b) Cu−1%CNT; (c) Cu−5%CNT; (d) Cu−10%CNT

the extruded specimen after etching the surface of the cross-section of the specimen. Sintering has been done well as a whole, and, in the case of the Cu specimen, particles are shown to be sintered along the same direction as that of extrusion. As in the result of observing the longitudinal section, some fine air pores are observed between the particles.

In the case of the Cu−CNT composite specimen, it has been confirmed that, if the CNT fraction increases, the specimen is sintered maintaining the particle form rather than the orientation. Through this, the CNT has an effect on particle size.

3.4 Indentation test measurement result

Figure 9 shows the stress−strain curves of specimens using the algorithm of indentation.

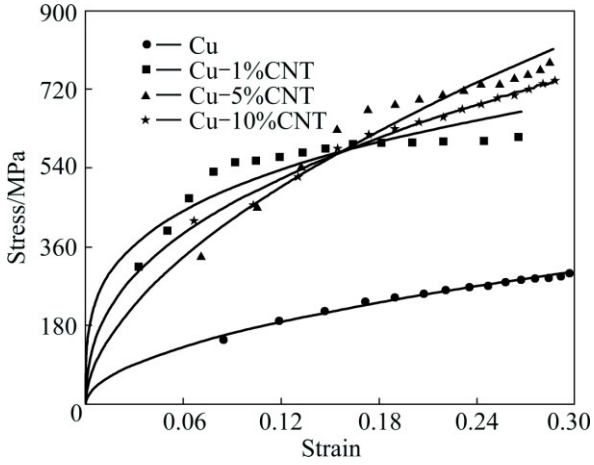

Fig. 9 Stress−strain curves of specimens

Figure 10(a) shows the hardness of the specimens. The hardness values increase on the whole when the content of added CNT is increased. The particles were refined when the nano powder was re-sintered, resulting in an increase in hardness.

In the case of the specimens made by adding CNT to Cu, the hardness increased more than 4 times, showing HV 209, HV 221 and HV 239 for 1% CNT, 5% CNT and 10% CNT, respectively, which was a gradual increase as the CNT fraction increased. The hardness values are thought to have increased from that of the original Cu as the CNT particles are distributed over the Cu particles [4].

Figure 10(b) shows yield strength on the surface by indentation test. Each specimen was measured six times, and the average value is illustrated. The yield strengths of Cu, Cu−1%CNT, Cu−5%CNT and Cu−10%CNT were measured to be 119.2, 249.9, 297.8 and 350 MPa, respectively.

Figure 10(c) shows the ultimate tensile strengths, which were 463.9, 863.7, 1026.7 and 1463.1 MPa, respectively, showing a similar trend. The tensile strength and yield strength showed an increasing trend as the CNT fraction increased, and the specimens containing CNT showed high values, typically more than twice that of the Cu specimen. This seems to be the effect of adding CNT, which has excellent mechanical properties, on the strength of Cu. It is necessary to conduct additional tests in order to find out the optimum CNT fraction to be added.

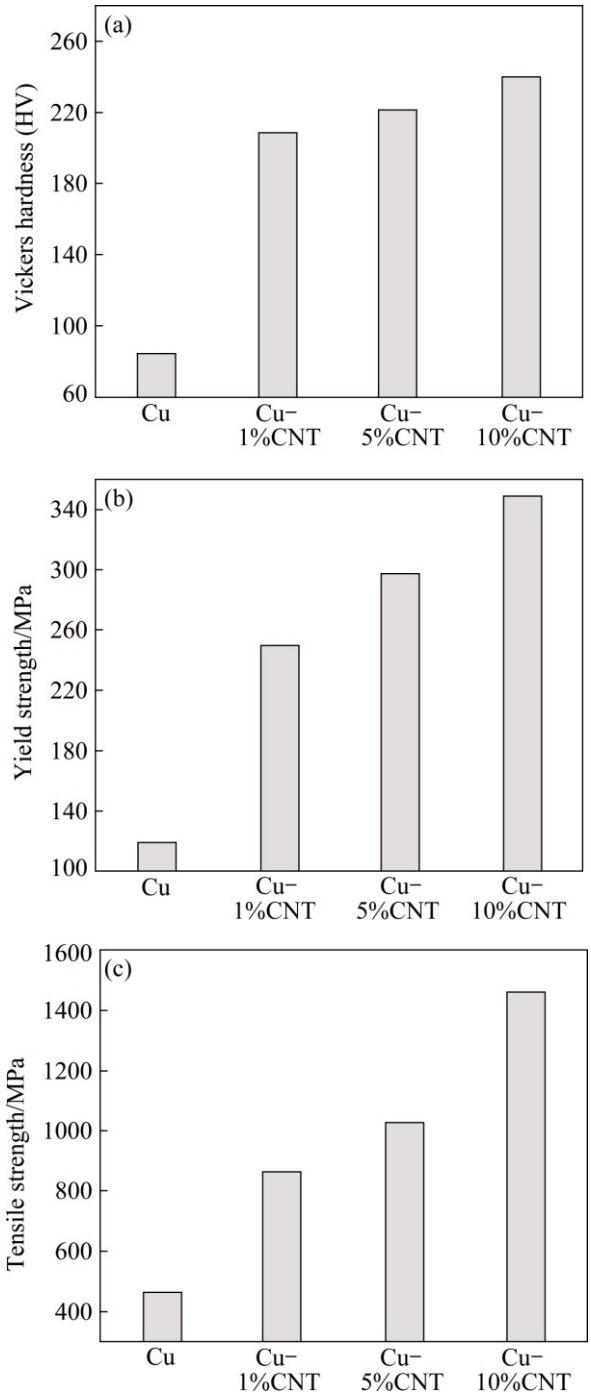

Fig. 10 Results of indentation test: (a) Hardness; (b) Yield strength; (c) Ultimate tensile strength

4 Conclusions

1) As a result of measuring the particle size of PSD, the particle size of the powder containing CNT increased by 5 times the particle size of the Cu powder. The particle size of the powder containing 10% CNT is smaller than that of the powder containing 5% CNT. A high CNT content rather interferes with crystal growth and it is important to mix a certain ratio of CNT.

2) As a result of observing the specimen using FE-SEM, sintering was achieved to form a grain boundary, and some air pores were observed in the specimen containing CNT. This is because of the effect of filling density.

3) As a result of indentation measurement, the hardness, tensile strength and yield strength increased as a whole due to the characteristics of nano powder and increasing CNT fraction.

Acknowledgments

This work was supported by the Gyeongsang National University Fund for Professors on Sabbatical Leave (2014) and Basic Science Research Program though the National Research Foundation of Korea (NRF) funded by the Ministry of Science, ICT and future Planning (2015R1A2A01004579).

References

[1] KWON H S, PARK D Y, LEE D Y, EUH K J, LEE K A. A study on the microstructure and physical properties of cold sprayed Cu/CNT composite coating [J]. Journal of the Korean Institute of Metals and Materials, 2008, 46: 182−188.

[2] IIJIMA S. Helical microtubules of graphitic carbon [J]. Nature, 1991, 354: 56−58.

[3] SUNG J H, RYU S R, LEE D J. Effects of strain-induced crystallization on mechanical properties of elastomeric composites containing carbon nanotubes and carbon black [J]. Transactions of the Korean Society of Mechanical Engineers A, 2011, 35: 999−1005.

[4] OH S Y, LIM B S, KIM C J, KIM B J, SUNG B H, BAIK S H. The properties of copper matrix nano composites using nickel-coated carbon nano-tube [J]. The Korean Society of Mechanical Engineers, 2008, 28: 144−147.

[5] KIM P, SHI L, MAJUMDAR A, MCEUEN P L. Thermal transport measurements of individual multiwalled nanotubes [J]. Physical Review Letters, 2001, 84(20): 215502-1−4.

[6] YU C, SHI L, YAO Z, LI D, MAJUMDER A. Thermal conductance and thermopower of an individual single-wall carbon nanotube [J]. Physical Review Letters, 2005, 5(9): 1842−1846.

[7] FRANK S, PONCHARAL P, WANG Z L, HEER W A. Carbon nanotube quantum resistors [J]. Science, 1998, 280: 1744−1746.

[8] ESAWI A M K, MORSI K, SAYED A, TAHER M, LANKA S, Effect of carbon nanotube (CNT) content on the mechanical properties of CNT-reinforced aluminium composites [J]. Composites Science and Technology, 2010, 70: 2237−2241.

[9] SELVAKUMAR P, BHATNAGAR N. Studies on polypropylene/ carbon fiber composite foams by nozzle-based microcellular injection molding system [J]. Materials and Manufacturing Processes, 2009, 24: 533−540.

[10] KIM D S, RAHMAN K, KHAN A, CHOI K H. Direct fabrication of copper nanoparticle patterns through electrohydrodynamic printing in Cone-Jet mode [J]. Materials and Manufacturing Processes, 2012, 27(12): 1295−1299.

[11] ALBERTO L G, IGNACIO R R, RUBEN V H, ROBERTO A B C, ANTONIO S G, ANDRES H R, MARIO ER G. Synthesis of copper-alumina composites by mechanical milling: An analysis [J]. Materials and Manufacturing Processes, 2013, 28(2): 157−162.

[12] ZHU C, WANG C, LANG J, MA Y, MA N. Si-Coated diamond particles reinforced copper composites fabricated by spark plasma sintering process [J]. Materials and Manufacturing Processes, 2013, 28(2): 143−147.

[13] DAREN L, ZUYAN L, YANG Y, ERDE W. Research on the densification of W−40wt% Cu by liquid sintering and hot-hydrostatic extrusion [J]. International Journal of Refractory Metals and Hard Materials, 2008, 26: 286−289.

[14] MORSI K, ESAWI A M K, LANKA S, SAYED A, TAHER M. Spark plasma extrusion (SPE) of ball-milled aluminum and carbon nanotube reinforced aluminum composite powders [J]. Composites Part A: Applied Science and Manufacturing, 2010, 4: 322−326.

[15] RLEE K Y, HAN W Y, PARK H J, KIM S S. Fabrication of aluminum/copper clad composite using hot hydrostatic extrusion process and its material characteristics [J]. Materials Science and Engineering A, 2004, 384: 70−76.

[16] KIM S W, CHUNG W S, SOHN K S, SON C Y, LEE S H. Fabrication and fracture properties of alumina matrix composites reinforced with carbon nanotubes [J]. Journal of the Korean Institute of Metals and Materials, 2009, 47(1): 50−58.

[17] CHU K, GUO H, JIA C C, YIN F Z, ZHANG X M, LIANG X B, CHEN H. Thermal properties of carbon nanotube-copper composites for thermal management applications [J]. Nanoscale Research Letters, 2010(5): 868−874.

[18] KWON H, ESTILI M, TAKAGI K, MIYAZAKI T, KAWASAKI A. Combination of hot extrusion and spark plasma sintering for producing carbon nanotube reinforced aluminum matrix composites [J]. Carbon, 2009, 47: 570−577.

[19] JEON E C, PARK J S, CHOI D S, KIM K H, KWON D I. A method for estimating uncertainty of indentation tensile properties in instrumented indentation test [J]. Journal of Engineering Materials and Technology, 2009, 131: 031006-1−6.

挤压工艺制造铜基复合材料的力学性能

Ji-Hun PAK[1], Gwi-Nam KIM[1], Sung-Gu HWANG[1], Beom-Su KIM[2], Jung-Pil NOH[3], Sun-Chul HUH[3]

1. Department of Mechanical and Precision Engineering,
Gyeongsang National University, Tongyeong 53064, Korea;
2. Department of Mechanical System Engineering, Gyeongsang National University, Tongyeong 53064, Korea;
3. Department of Mechanical and Energy Engineering, Gyeongsang National University, Tongyeong 53064, Korea

摘　要：碳纳米管因具有优异的电学、力学和热力学性能而被应用于各个领域。利用挤压工艺球磨 Cu−CNT 粉末制造复合材料，根据 CNT 的含量评估 Cu−CNT 复合材料的力学性能。采用行星式球磨机在 500 r/min 下混合分散 CNT (1%, 5% 和 10%)、铜(d=100 nm)、氧化锆球(90 g)和乙醇(20 mL) 5 min。用铜制造直径 50 mm、长 100 mm 的坯锭，在单轴压力下将复合材料粉末填入坯锭。在挤压过程中，坯锭在 880 °C 下加热 1 h 后，坯锭负载 200 t，得到圆棒状样品。采用粒度分布仪测量复合材料的粒度，同时采用 SEM 观察挤压样品的表面组织。使用压痕仪测量的力学性能随着 CNT 含量的增加而提高。Cu−CNTs 复合材料的屈服强度、抗拉强度和硬度明显提高。

关键词：碳纳米管；挤压；球磨；压痕；基体；力学性能；显微组织

(Edited by Xiang-qun LI)